

NOAA Award Number: NA13OAR4590192
Program Officer: Richard Fulton ,301-734-1289, Richard.Fulton@noaa.gov
Program Office: OAR Office of Weather and Air Quality (OWAQ)
Award Period: 09/01/2013 - 08/31/2015
Project Title: Improving the GFDL/GFDN Operational Tropical Cyclone Models at NOAA/NCEP and Navy/FNMOC
Recipient Name: University of Rhode Island
PIs/PDs: Isaac Ginis and Morris Bender
Report Type: Project Progress Report
Reporting Period: 03/01/2015 - 08/31/2015
Final Report: Yes

In this final report, we summarize the main results accomplished during this two-year project and the upgrades implemented into the operational GFDL and GFDN models for the 2014 and 2015 seasons.

1. Atmospheric model resolution, initialization and physics upgrades

Through JHT funding, major upgrades have been finalized at the National Centers for Environmental Prediction (NCEP) for operational implementation of the new high-resolution version of the GFDL hurricane model. The inner nest resolution has increased from 9 to 6 km, which is the highest resolution possible for a hydrostatic model. The surface exchange coefficients (C_h and C_d) have been reformulated consistent with some of the recent referred studies (Fig. 1) (Edson et al. 2013, Andreas 2011, Soloviev et al. 2014). In addition, the ocean currents are now taken into account in the surface stress computation.

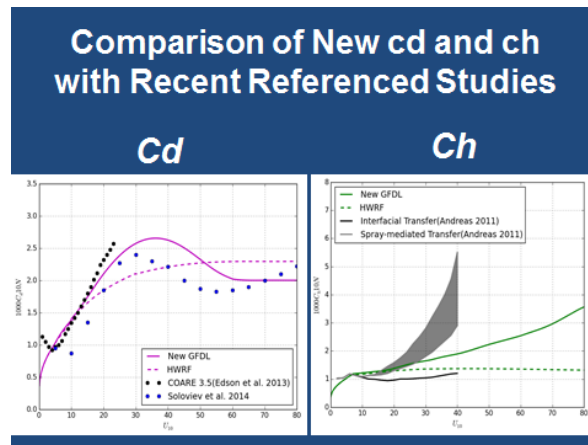


Figure 1. Plot of the new C_d (left, purple line) compared to the old version operational in both GFDL and HWRf (purple dashed line) and to estimates from observational data (black dots) and a recent theoretical study (blue dots). Also shown (right) is the formulation of the new C_h (solid green) compared to the 2014 version operational in HWRf (green dashed) and theoretical studies by Andreas (2011).

Additional model upgrades included modification of the Planetary Boundary Layer (PBL) and surface layer using the critical Richardson number, advection of the individual microphysics species, and improved targeting of the storm maximum wind and storm radius in the vortex initialization. Advection of the rime factor was also evaluated but not included because impact was minimal.

The new model configuration was extensively tested for most of the storms during the 2008 and 2010-2012 Atlantic seasons, as well as the 2011-2013 Eastern Pacific seasons. Results indicated significantly reduced intensity errors, particularly in the Atlantic basin (Fig. 2). For the Atlantic, the reduction of wind intensity errors averaged nearly 15% at days 3-5 and about 6% at the shorter forecast lead times. For the Eastern Pacific, improvements averaged about 5 to 8%. Another measure of improved model performance is the percent of storms that had overall improved intensity guidance compared to the current version. As seen in Fig. 3, compared to the previous operational GFDL model, over 80% of the Atlantic storms had better intensity guidance for the 3-5 day forecast lead times, and about 60% of the storms had improved guidance at the earlier forecast times.

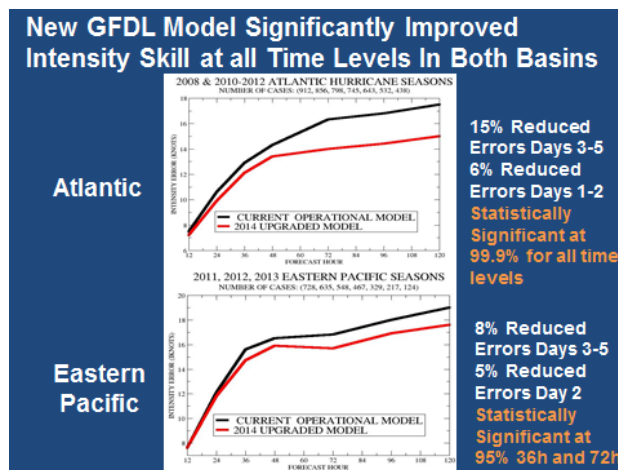


Figure 2. Average intensity errors for the Atlantic (top) and Eastern Pacific (bottom) for all forecast time periods for the selected storms used in the evaluation of the new model (red line), compared to the previous version used in operations at NCEP (black line).

The biggest impact on intensity was a large reduction in the over-intensification of weaker storms (Fig. 3), greatly reducing the model’s positive bias for these non-intensifying systems.

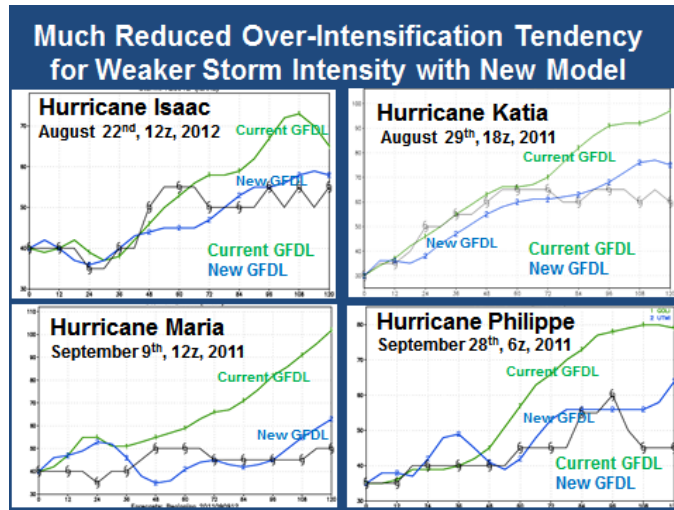


Figure 3. Time series of forecasted maximum surface winds with the upgraded GFDL model (blue) compared to the previous operational model (green) for the forecast of four Atlantic storms.

Increase in the number of vertical levels in the GFDL hurricane model from 42 to 60 vertical sigma levels, was tested and carefully evaluated for over 600 cases in the Atlantic and 300 cases in the Eastern Pacific. The configuration selected was nearly identical to the HWRF vertical configuration with two differences (lowest model level of the current operational GFDL model was retained and an additional vertical level was added to the upper troposphere). The radiation code in the current operational model was modified and fully generalized to run from any specified vertical sigma level distribution. Although the impact was mostly positive in the Atlantic, the increased resolution resulted in increased negative bias for intense hurricanes and this upgrade was rejected for operational implementation.

In the previous GFDL hurricane forecast system, the resolved vortex in the initial global analysis was removed and replaced with a model consistent vortex that was spun up during a 60 hour integration of an axisymmetric version of the 3D hurricane model. The tangential component of the wind was gradually forced toward a profile obtained from the operational tvitals file, while the remaining prognostic variables evolve in a model consistent way. Additional analysis made during this project indicated that the initial vortex often had too low humidity for weak storms. The reason was the methodology of spinning up the initial moisture field (r) from an environmental value determined beyond the filter domain of the global vortex (Equation 1), which was dryer than in the storm region. A better strategy that was considered and tested was to replace the environmental moisture with the value from the global analysis, and add in the moisture deviation computed relative to this value (Equation 2) instead of the previous environmental moisture field. This resulted in a much more reasonable initial moisture field, as shown in Fig. 4 for one case of Hurricane Earl. Even by forecast hour 42 (Fig. 4, bottom left), the moisture in the middle troposphere was still anomalously dry compared to the revised moisture initialization method (bottom right), which resulted in underprediction of storm intensity (blue line, Fig. 5). Since this problem was worse for weak storms in the old operational system, the vortex initialization was not run in 2014 for storms of 40 knots or less, to enable better intensification for rapid developing cases (red line, Fig. 5). However with the improved

moisture initialization, the intensity is much better forecasted (green line, Fig. 5) and the vortex initialization was introduced again in 2015 for all systems regardless of intensity.

$$(U, V, T, r, p^*) = (U, V, T, r, p^*)_{\text{Envr}} + (U, V, T, r, p^*)_{\text{axi-sym vortex}} \quad (1)$$

$$(U, V, T, p^*) = (U, V, T, p^*)_{\text{Envr}} + (U, V, T, p^*)_{\text{axi-sym vortex}} \quad (2)$$

$$r = r_{\text{gfs}} + r_{\text{vortex}}$$

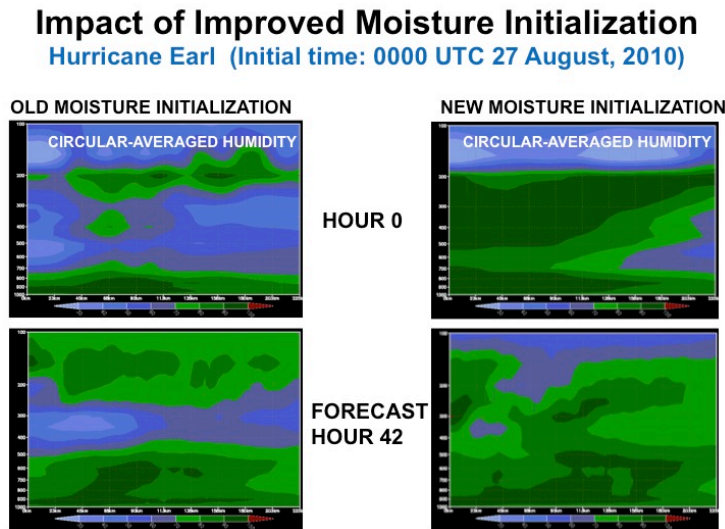


Figure 4. Circular-averaged cross-sections of relative humidity at hour 0 (top) and forecast hour 42 (bottom), for one case of Hurricane Earl (2010) using the moisture initialization procedure (left) used in the old operational GFDL forecast system, and the new system (right).

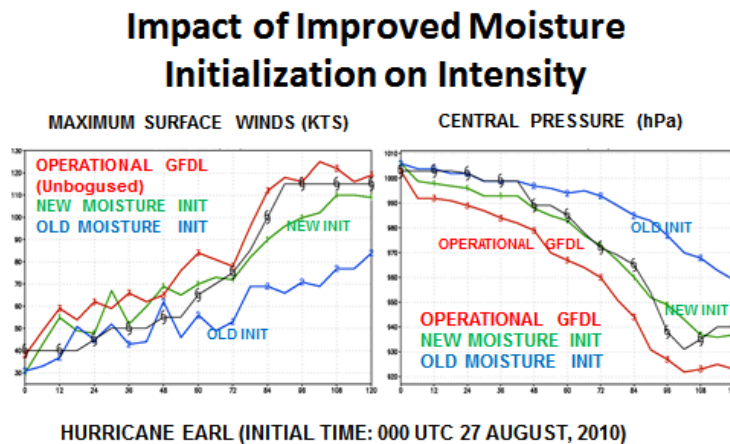


Figure 5. Time series of central pressure (left) and maximum surface wind (right) for the case of Hurricane Earl predicted in the current operational GFDL model (red, which is run without bogusing), compared to the forecast using the previous bogusing initialization procedure (blue) and the improved moisture initialization procedure (green).

In the operational GFDL initialization, an important parameter used in the axisymmetric vortex spinup, is the radial extent of the storm (R_b) defined as the radius where the positive tangential winds go to zero. During the spinup, the tangential wind is targeted toward a storm profile determined by the reported wind radii from the operational tcvitals file. In the old system, R_b was assumed to be a function of the reported radius of the last closed isobar RCLI (e.g., $R_b = 1.5 * RCLI$). Examining the performance of the Navy's operational version of the GFDL model (GFDN) for the 2013 Western Pacific season, it was found that the track and intensity was significantly degraded in some of the forecasts, due to too small reported RCLI compared to the observed satellite estimates (e.g., Knaff, personal communication). A new formulation independent of RCLI was developed. It is based on the assumption that absolute angular momentum $M(r)$ is roughly conserved for a parcel moving inwardly toward the storm center from R_b . Following the methodology outlined in Carr and Elsberry (1997), the following formula was derived for R_b , and tested throughout most of the 2014 Western Pacific system in near real time, in a parallel version of the GFDL model run on the JET supercomputer facility using the NCEP (National Centers for Environmental Prediction) GFS (Global Forecast System) analysis:

$$(R_b) = e^{(MLG/(1+x))}$$

where

$$MLG = \log(2(M(r)_{gale} / f r_{gale}^{(1-x)}))$$

The expression $M(r)_{gale}$. Absolute angular momentum of the storm at the radius of the gale force winds is defined as:

$$M(r)_{gale} = r_{gale} v_{gale} + \frac{1}{2} f r_{gale}^2$$

where r_{gale} is computed as the average of the 4 gale force wind radii reported from the tcvitals file and x is a scaling factor set to 0.4, as suggested by Carr and Elsberry (1997).

The operational GFDL model was tested for tropical cyclones during the 2011, 2012 and 2014 Atlantic seasons with the above mentioned changes using the new version of the GFS made operational at NCEP in 2014. Due to the limitations in disc storage needed to run these tests using the new high resolution GFS, it became impractical to run every storm for this multi-year sample. Nevertheless, a sample size of 638 cases (which contained all of the significant tropical systems during that period) was considered sufficient to evaluate the performance for both the 60 level and 42 level versions of the upgraded GFDL system. Results are shown in Fig. 6 for the interpolated forecasts (early guidance), to exactly represent the version that is available to the operational hurricane forecasters in real time.

Impact on track was mostly neutral for this multi-year sample size, although both versions of the model had about 3% reduced error in the critical 2-3 day forecast lead times, with a slightly more reduced error of about 5% at days 4-5 with the 60 level model. However, these improvements were still statistically significant at the 96% level for all forecast lead times for the 60 level

model compared to the current model, except forecast hour 36h. For the late model guidance (not shown) statistical significance was also obtained for the 42 level model through forecast hour 72. For intensity, the improvement was much more significant, with reduced intensity errors averaging about 11% for the 42 level model for the first 36h, compared to the 60 level version. However in the later forecast time periods the 60-level model performed better, with an average reduction in intensity errors of 10% compared to the 42 version.

2011, 2012, 2014 Atlantic Seasons with New GFS

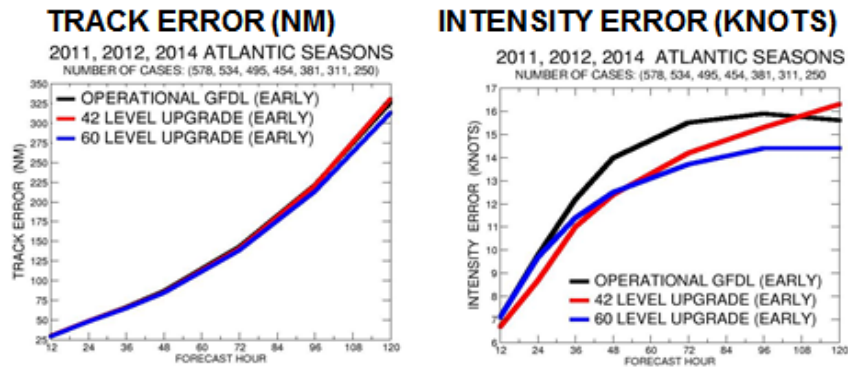


Figure 6. Average track error (left) and intensity error (right) for storms from the 2011, 2012, and 2014 Atlantic hurricane season, comparing the previous operational GFDL model (black), with the 42 level (red) and 60 level (blue) upgraded GFDL. All of the results shown are for the early model interpolated guidance and all forecasts are run off of the new GFS.

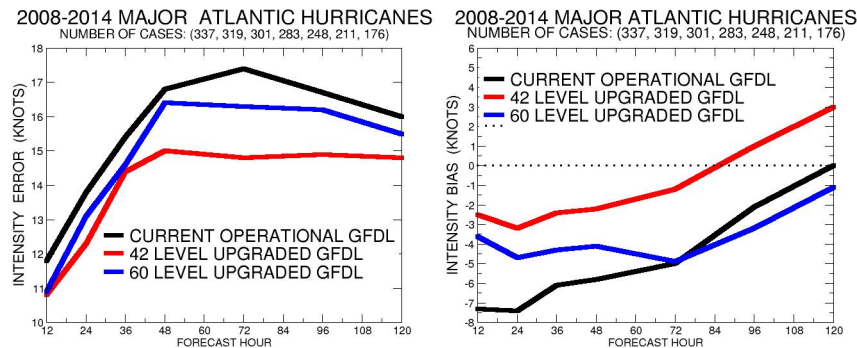


Figure 7. Average intensity error (left) and intensity bias (right) for major hurricanes during the 2008-2014 Atlantic Hurricane seasons, comparing the previous operational GFDL model (black) and the 42 level and 60 level upgraded GFDL model (blue and red lines). The storms during the 2008 and 2010 seasons (*Ike, Danielle, Earl, Igor and Julia*) were run using the old GFS background fields, while the storms run during the 2011-2014 seasons (*Irene, Katia, Edouard and Gonzola*) were run using the new GFS fields.

Although the results outlined above for the 60 level upgraded version of the GFDL hurricane model were promising, closer evaluation raised several concerns about upgrading the model vertical resolution in 2015, as originally planned. The multi-year sample upon which these tests

were performed had only a few major hurricanes and only one category 4 hurricane (Gonzolo, 2014). The intensity of Gonzolo (not shown) was very poorly predicted with the 60 level model, with an average error of 23 and 18 knots at 48 and 72 hours, compared to 20 and 14 knots for the current operational model, and 15 and 11 knots for the 42 level upgraded model. This was due to an average negative intensity bias of over -20 knots in the 60 level model during the 1-3 day forecast time period, compared to -17 and -14 knots for the operational and 42 level upgraded models, respectively.

For Hurricane Edouard, an excessive negative bias was also noted compared to the 42 level model. When additional tests were made on major hurricanes during the 2008-2014 seasons (Fig. 7) using both the new and old GFS, it was found that the intensity prediction (left) and bias (right) using the 60 level upgraded model (blue) was unacceptably degraded compared to the 42 level model (red) which had much reduced negative bias and improved intensity prediction compared to both the current operational model (black) and the 60 level version.

Hurricane Gonzalo (0000 UTC 13 October)

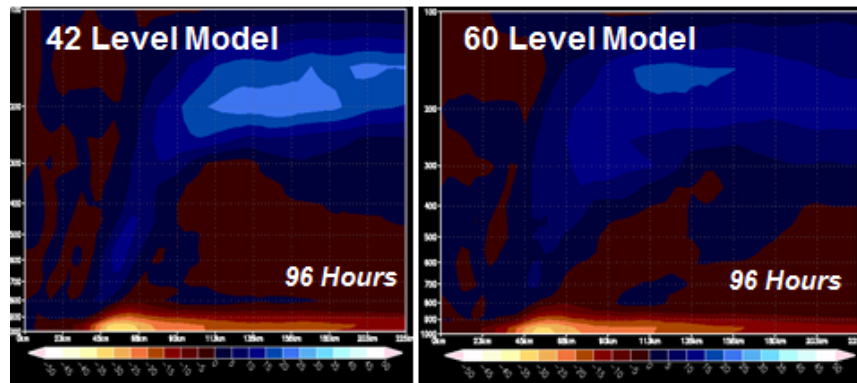


Figure 8. Circular-averaged cross-section of radial component of the wind for the upgraded 42 level (left) and 60 level (right) GFDL hurricane model, at forecast hour 96 for Hurricane Gonzalo initialized at 0000 UTC 13th October, 2014. Forecasts were run using the new GFS fields.

A number of likely reasons were found for this excessive negative bias. Analysis indicated that even for storms of comparable intensity, the secondary circulation and upper level outflow was typically weaker with the 60 level model with increased vertical resolution (Fig. 8). This result was consistent with Zhang et.al (2015), who found a weaker secondary circulation and reduced outflow with increased vertical resolution in the hurricane outflow region, for idealized simulations using Hurricane WRF (HWRF). This also negatively impacted the intensification in their simulations. Additional evaluation of different distributions of vertical sigma levels is needed to reduce this tendency, possibly reducing the number of levels in the outflow region, as suggested by Zhang et al. (2015) and adding more vertical levels in the middle troposphere, where the impact on the storm steering is greatest.

Another source of the increase negative bias in the 60 level model is reduced sea surface temperatures (SST) in the 60 level version of the upgraded model compared to the 42 level model (Fig. 9, bottom). The primary source of this is likely due to decreased amounts of solar

radiation reaching the ocean surface possibly related to increased amounts of ice in the upper troposphere (Fig. 9, top) as well as increased humidity and cloudiness in the upper boundary layer (not shown) at around 800 hPa, with the 60 level model. To help remedy this problem, evaluation of the 60 level GFDL model with enhanced turbulence diffusion in stratocumulus regions introduced in the GFS is currently being evaluated.

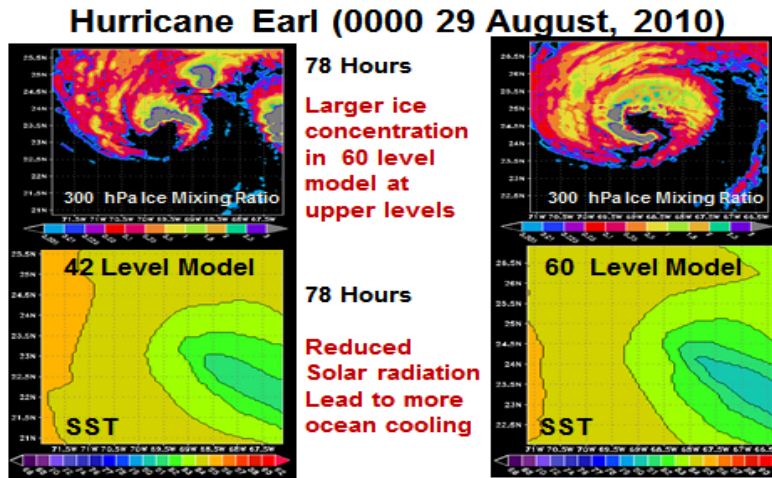


Figure 9. Horizontal distribution in the innermost nest for the 300 hPa ice mixing ratio (top) and SSTs (bottom) comparing the 42 level model (left) and 60 level model (right) at forecast hour 78 for Hurricane Earl initialization at 0000 29 August, 2010. Both forecasts are run using the new GFS fields.

2. Transition MPIPOM-TC to operations in all worldwide ocean basins

URI's new MPIPOM-TC ocean model with $\sim 1/12^\circ$ grid spacing was successfully transitioned to the operational GFDL model (as a replacement for POM-TC with $\sim 1/6^\circ$ grid spacing). This upgrade also replaced the two overlapping POM-TC ocean domains in the Western and Eastern Atlantic with a new, expanded transatlantic domain to prevent loss of ocean coupling for storms that move quickly from west to east or east to west in the central Atlantic (Fig. 10).

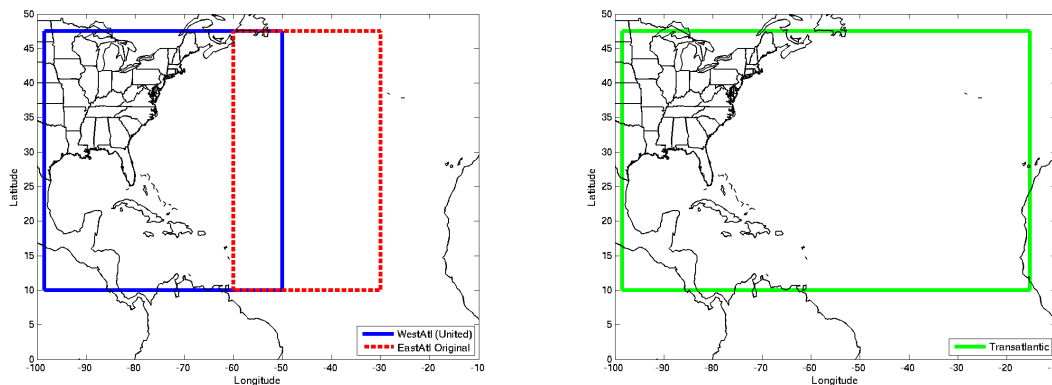


Figure 10. POM-TC's overlapping Western and Eastern Atlantic domains (left) and MPIPOM-TC's expanded transatlantic domain (right).

One of the goals of this project was to incorporate URI's new MIPOM-TC ocean model with $\sim 1/12^\circ$ grid spacing and flexible initialization options into the GFDL and GFDN models worldwide. In the upgraded operational GFDL/GFDN version MIPOM-TC replaces the old ocean model, POM, in all ocean basins. In order to extend MIPOM-TC capabilities worldwide, the computational domains have been designed to be relocatable to regions around the world. These regions include the Transatlantic, East Pacific, West Pacific, North Indian, South Indian, Southwest Pacific, Southeast Pacific, and South Atlantic domains (Fig. 11). Domain overlap helps to prevent loss of ocean coupling. To avoid domain-specific code, all worldwide domains were set to the same size: 869 (449) longitudinal (latitudinal) grid points, covering 83.2° (37.5°) of longitude (latitude) and yielding a horizontal grid spacing of ~ 9 km.

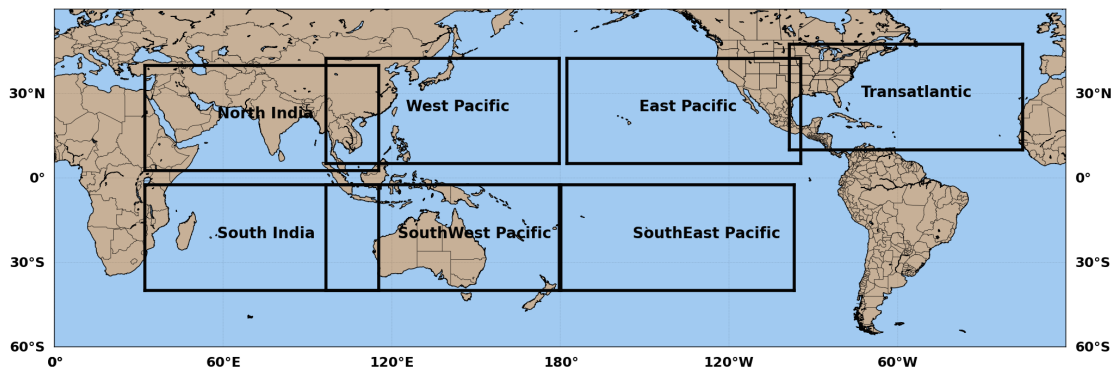


Figure 11. MIPOM-TC worldwide ocean domains.

The new MIPOM-TC ocean domains can be initialized from a variety of ocean initial conditions by simply utilizing a given “prep” module that has been developed for this purpose. All ocean initial conditions have the ability to assimilate the daily GFS or NAVGEM SST into the upper ocean mixed layer. For the 2014 operational GFDL model, MIPOM-TC is initialized with the feature-based prep module in the Transatlantic domain (fbtr) and the GDEMv3 monthly climatology prep module in the East Pacific domain (g3ep); both of these initializations were set to assimilate the GFS SST, as in the POM-TC initialization for the operational GFDL model prior to 2014. For the upgraded global GFDL/GFDN system the initial condition modules for MIPOM-TC have been developed using the stand-alone Navy Ocean Data Assimilation (NCODA) daily T and S fields (Cummins 2005) and versions of the HYbrid Coordinate Ocean Model (HYCOM) that use NCODA (Chassignet et al. 2009).

Fig. 12 shows the track and intensity forecasts for Hurricane Edouard initialized on September 12, 00Z using three different ocean products. It is interesting to note that the track forecast is most accurate with the NCODA ocean initialization, while the intensity prediction is most accurate using the feature-based initialization.

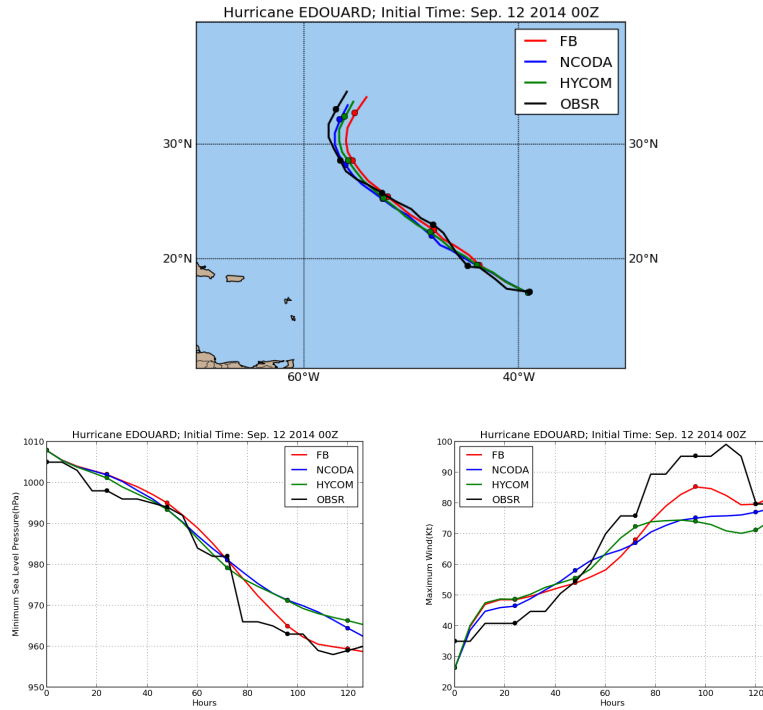


Figure 12. The GFDL track and intensity forecasts for Hurricane Edouard (Initial time: September 12, 00Z) in which the ocean model is initialized from different ocean products (red – feature-based, blue – NCODA, green – HYCOM).

Examples of using two different ocean initial condition options in simulating MPIPOM-TC’s ocean response to Super Typhoon Bolaven (West Pacific) and Cyclone Phailin (North Indian), using forcing from observed winds derived from the NHC message file (i.e. TC vitals) are shown in Figs. 13 and 14. The SST cold wakes produced by these tropical cyclones are evident, but the details of the cold wakes depend on the pre-storm SST initial conditions and the subsurface ocean initial conditions.

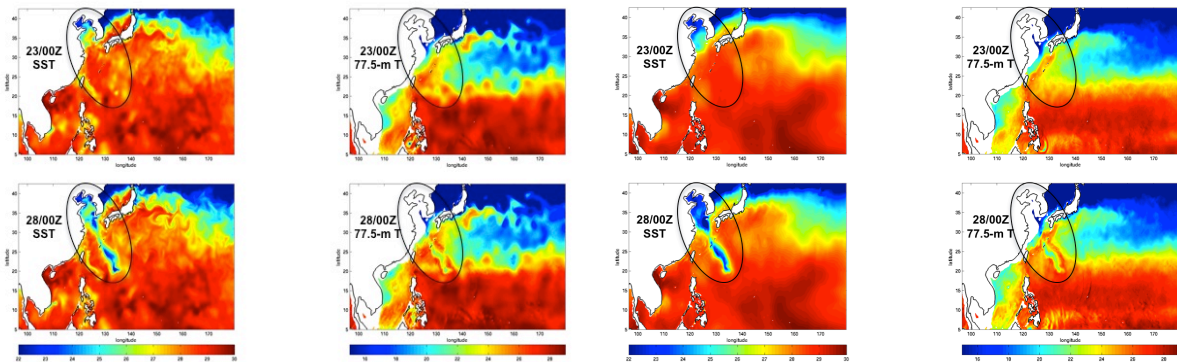


Figure 13. MPIPOM-TC’s ocean response to West Pacific Supertyphoon Bolaven’s observed wind forcing from 20120823 at 00Z to 20120828 at 00Z using the NCODA (left four panels) or GDEMv3 + GFS SST (right four panels) initial condition: SST at 23/00Z; 77.5-m T at 23/00Z; SST at 28/00Z; 77.5-m T at 28/00Z.

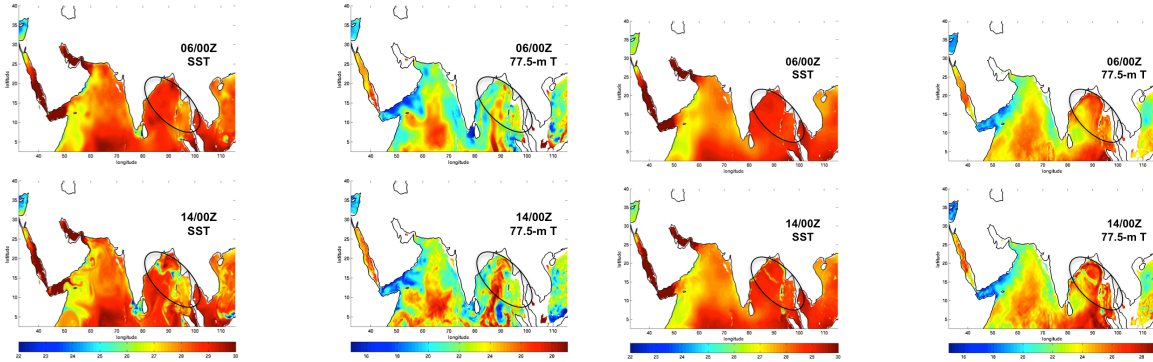


Figure 14. MPIPOM-TC's ocean response to North Indian Cyclone Phailin's observed wind forcing from 20131006 at 00Z to 20131014 at 00Z using the NCODA (left four panels) or GDEMv3 + GFS SST (right four panels) initial condition: SST at 06/00Z; 77.5-m T at 06/00Z; SST at 14/00Z; 77.5-m T at 14/00Z.

The new global MPIPOM-TC ocean scripts have been successfully implemented into the GFDL real-time ensemble forecast system run on the Jet computer and now world-wide forecasts are available to the JTWC forecasters.

3. Transitioning the upgraded GFDN to operations at FNMOC

During this project the upgraded GFDN forecast system has been successfully transitioned to operations at FNMOC. Fig. 15 shows the intensity forecast errors and bias of the upgraded GFDN in the western Pacific since August 17, 2015. GFDN has now quite comparable skill to other regional models with much improved track skill compared to the previous version (not shown). We identified the main reason for the still quite large negative intensity bias. It is caused by using the NCODA data for ocean model initialization, which causes excessive cooling in the cold wake, probably due to a too shallow representation of the mixed layer. The GFDL system, which runs off the GFS global model, uses GDEM ocean monthly climatology with SST assimilation instead (Yablonsky and Ginis, 2008) which contributed to more intensity skill and much less negative bias compared to GFDN, as seen in Fig. 15. When GDEM was replaced with NCODA in GFDL it showed an increased negative bias, similar to GFDN (figure not shown).

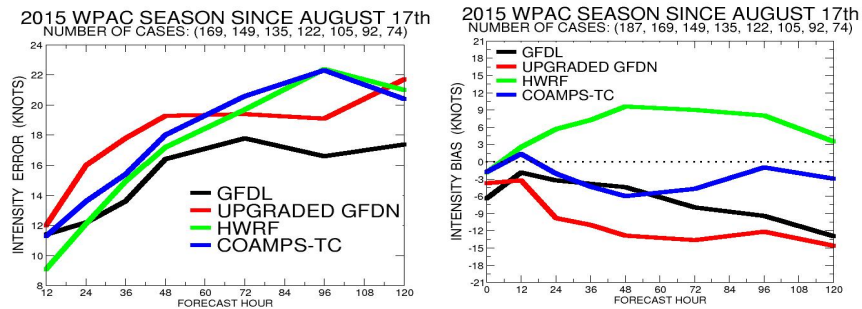


Figure 15. The upgraded operational GFDN intensity forecast errors and bias compared to other regional models in the western Pacific since August 17, 2015.

In order to implement the GDEM climatology into GFDN, it is required to use the Navy's version of GDEM. We therefore conducted evaluation and comparison of the two GDEM data products. Fig. 16 shows comparison of the temperatures at the sea surface and at a depth of 50 m. The Navy's version is a little colder to the north at higher latitude and warmer at lower latitudes. The differences in the intensity predictions are found to be generally small, as shown in Figure 17. Based on this evaluation, Navy's version of GDEM has been transition to the GFDN operational system.

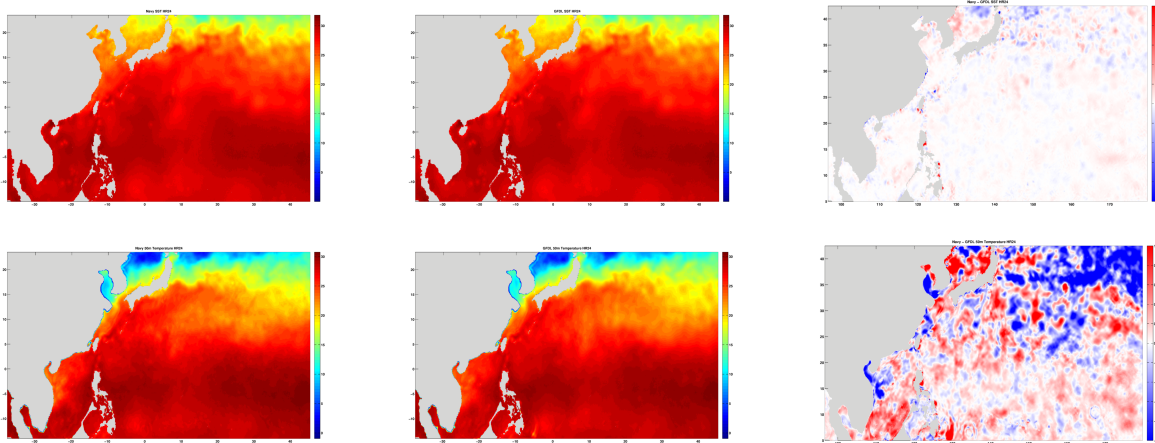


Figure 16. Comparison of Navy GDEM (left), GFDL GDEM (center), and difference (right) at the sea surface (top) and at 50 m depth (bottom).

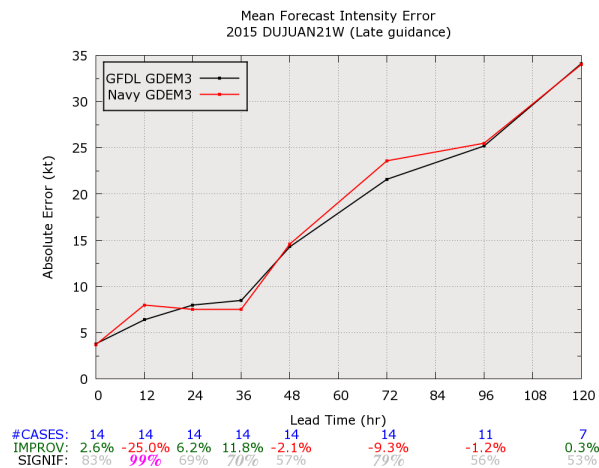


Figure 17. Evaluation of the impact of using Navy and GFDL versions of GDEM on the tropical cyclone intensity prediction for 14 forecasts of Typhoon DUJUAN (21W).

4. Improving and evaluating the explicit wave coupling in the GFDL model

We have continued to improve and evaluate the experimental GFDL/WAVEWATCH III/MPIPOM-TC system. In the three-way air-wave-sea coupled framework, which is based on a comprehensive, physics-based treatment of the wind-wave-current interaction, the bottom boundary condition of the atmospheric model incorporates sea-state dependent air-sea fluxes of momentum, heat, and humidity, and it includes the effect of sea-spray. The wave model is forced by the sea-state dependent wind stress and includes the ocean surface current effect. The ocean model is forced by the sea-state dependent wind stress and includes the ocean surface wave effects (i.e. Coriolis-Stokes effect, wave growth/decay effect).

We have incorporated two different wind stress parameterization schemes, one based on Donelan et al. (2012) and the other based on Reichl et al. (2014). In addition, we adjusted the behavior of the drag as a function of wind speed to be consistent, on average, with the C_d formulation implemented in the 2014 operational GFDL model. Examples of the spatial distribution of the drag coefficient under a typical (idealized) TC are shown in Fig. 18 (top panels). Although the wind speed is nearly axisymmetric, the drag coefficient significantly varies depending on the location relative to the hurricane center. In particular, the drag coefficient is significantly reduced in the front right quadrant in both parameterizations. The sea state dependence of the drag coefficient at different wind speeds is shown in Fig. 18 (bottom panels). The sea state dependence is enhanced most significantly at higher wind speeds.

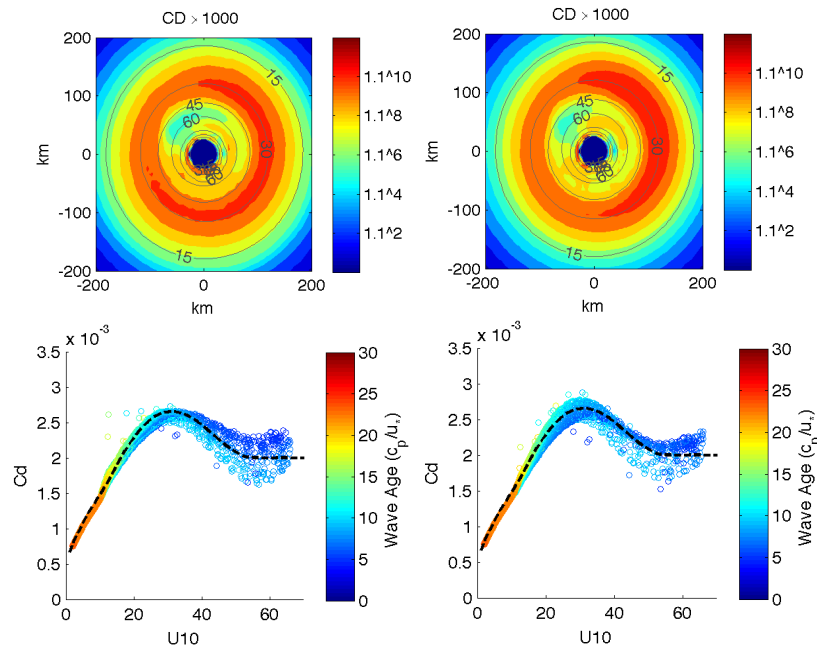


Figure 18. 10-meter neutral drag coefficient for an idealized tropical cyclone with a radius of maximum wind of 50 km and a maximum wind speed of 65 m/s. The top panel shows spatial distributions. The tropical cyclone is moving from right to left at 5 m/s. The bottom panels show sea state dependence of the drag coefficient at different wind speeds. Left panels: Donelan et al. (2012) drag coefficient; Right panels: Reichl et al. (2014) drag coefficient.

We have begun careful evaluation of the new GFDL system for real hurricane simulations. Fig. 19 shows the track and intensity prediction of Hurricane Irene (Initial time: Aug. 22, 2011 12Z). With the wave coupling, both the track and intensity forecasts are noticeably improved. Fig. 20 shows the simulated significant wave height at 72 hr and SST. It is interesting to note the differences in the spatial distribution and magnitude of the cold wake in the simulations with (left) and without (right) wave coupling.

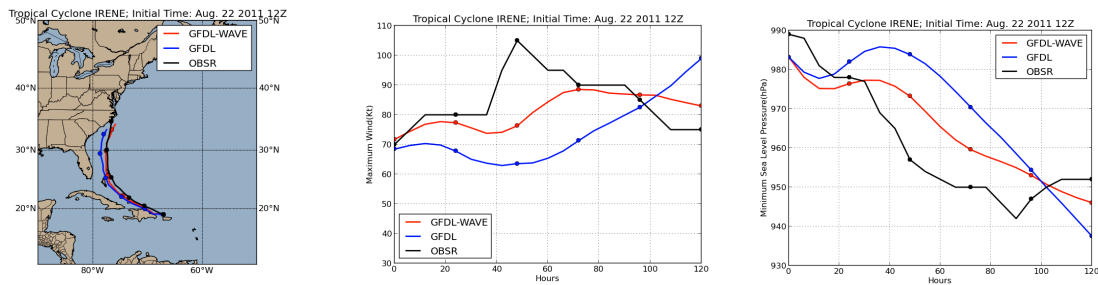


Figure 19. Track and intensity prediction of Hurricane Irene (Initial time: Aug 22, 2011 12Z) with the new GFDL hurricane-wave-ocean system in comparison to the operational GFDL hurricane-ocean system and observations.

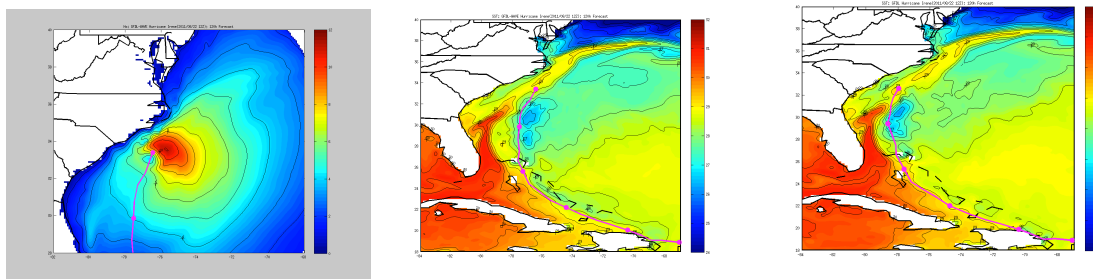


Figure 20. Significant wave height (left), SST ($^{\circ}\text{C}$) with the new GFDL hurricane-wave-ocean system and without wave coupling (right) at 72 hr of the Hurricane Irene (Initial time: Aug. 22, 2011 12Z).

References:

- Andreas, E. L., 2011: Fallacies of the enthalpy transfer coefficient over the ocean in high winds. *J. Atmos. Sci.*, **68**, 1435–1445.
- Carr, L.E. and R. L. Elsberry, 1997, Models of tropical cyclone wind distribution and beta-effect propagation for application to tropical cyclone track forecasting, *Mon. Wea. Rev.*, **125**, 3190-3209.
- Carnes, M. R., 2009: Description and evaluation of GDEM-V 3.0. Naval Research Laboratory, Stennis Space Center, MS 39529, 21 pp. [NRL/MR/7330--09-9165].
- Chassignet, E. P., H. E. Hurlburt, E. J. Metzger, O. M. Smedstad, J. Cummings, G. R. Halliwell, R. Bleck, R. Baraille, A. J. Wallcraft, C. Lozano, H. L. Tolman, A. Srinivasan, S. Hankin, P. Cornillon, R. Weisberg, A. Barth, R. He, F. Werner, and J. Wilkin, 2009: US GODAE:

- Global ocean prediction with the HYbrid Coordinate Ocean Model (HYCOM). *Oceanogr.*, **22**, 64-75.
- Cummings, J. A., 2005: Operational multivariate ocean data assimilation. *Quart. J. Royal Meteor. Soc.*, **131**, 3583-3604.
- Cummings, J. A., and O. M. Smedstad, 2013: Variational data assimilation for the global ocean. *Data Assimilation for Atmospheric, Oceanic and Hydrologic Applications*, Vol. II, S. Park and L. Xu, Eds., Springer, 303–343.
- Donelan, M. A., M. Curcic, S. S. Chen, and A. K. Magnusson, 2012: Modeling waves and wind stress. *J. Geophys. Res.*, **117**, C00J23.
- Edson, J. B., and Coauthors, 2013: On the Exchange of Momentum over the Open Ocean. *J. Phys. Oceanogr.*, **43**, 1589–1610.
- Jongil, H. and H. -L. Pan, 2011: Revision of convection and vertical diffusion schemes in the NCEP Global Forecast System, *Wea. Forecasting*, **26**, 520-533.
- Falkovich, A., I. Ginis, and S. Lord, 2005: Ocean data assimilation and initialization procedure for the Coupled GFDL/URI Hurricane Prediction System. *J. Atmos. Oceanic Technol.*, **22**, 1918-1932.
- Reichl, B. G., T. Hara, and I. Ginis, 2014: Sea state dependence of the wind stress over the ocean under hurricane winds. *J. Geophys. Res. Oceans*, **119**, 30-51.
- Soloviev A., R. Lukas, M. Donelan, B. Haus, and I. Ginis, 2014: The air-sea interface and surface stress under tropical cyclones, *Nature Scientific Reports*, **4**.
- Teague, W. J, M. J. Carron, and P. J. Hogan, 1990: A comparison between the Generalized Digital Environmental Model and Levitus climatologies. *J. Geophys. Res.*, **95**, 7167-7183.
- Zhang, D.L., L. Zhu, X. Zhang, V. Tallapragada, 2015, Sensitivity of idealized hurricane intensity and structures under varying background flows and initial vortex intensities to different vertical resolution in HWRF, *Mon. Wea. Rev.*, **143**, 914-932.
- Yablonsky, R. M., and I. Ginis, 2008: Improving the ocean initialization of coupled hurricane-ocean models using feature-based data assimilation. *Mon. Wea. Rev.*, **136**, 2592-2607.
- Yablonsky, R. M., I. Ginis, B. Thomas, 2015: Ocean modeling with flexible initialization for improved coupled tropical cyclone-ocean prediction, *Environmental Modelling & Software*, **67**, 26-30.